06,04

Relaxation processes in porous potassium sodium niobate ceramics

© O.V. Malyshkina[1], N.E. Malysheva[2], D.V. Mamaev[1]

[1] Tver State University,
Tver, Russia
[2] Military Academy of Aero-Space Defence named after Marshal of the Soviet Union G.K. Zhukov,
Tver, Russia

E-mail: Olga.Malyshkina@mail.ru

Received April 19, 2025
Revised April 28, 2025
Accepted April 28, 2025

Comparative studies of the experimental and calculated, based on a mathematical model, dielectric response of porous potassium sodium niobate (KNN) ceramics with a pore content of 10, 25 and 40 volume percent were carried out. Based on mathematical modeling, it is shown that in KNN samples without pores, the contribution to the dielectric response of relaxation conductivity is present only in the monoclinic phase (temperature range 200−400 °C). The presence of pores in KNN samples leads to the appearance of additional contributions of conduction processes to the dielectric response. In the experiments, this manifests itself as the appearance of additional (in comparison with a similar dependence for a sample without pores) linear segments on the dependence of the real part of the complex conductivity on the inverse temperature in Arrhenius coordinates. This indicates a set of activation energies and, as a consequence, the presence of various conductivity mechanisms in porous samples.

Keywords: piezoelectric ceramics, porous ceramics, potassium sodium niobate, dispersion of complex permittivity, relaxation processes, resonance polarization.

DOI: 10.61011/PSS.2025.05.61495.87-25

1. Introduction

Use of piezoelectric ceramics is driven by wide use of piezoelectric effect in various energy converters, surface acoustic wave (SAW) filters, sensors, drives, ultrasonic converters etc. Some features in the properties of porous ceramics indicate its exclusive fitness as a material for manufacturing of sensors used in medical diagnostics [1,2] and electromechanical converters in hydro-acoustics. Design of new modified ceramic compositions based on sodium niobate — is one of the predicted areas for development of piezoelectric ceramic not containing lead [3–7]. The authors [7] have shown that use of alkali metal niobates in the form of porous ceramic makes it possible to improve the main functional parameters of these materials and makes them competitive to piezoceramics of the lead zirconate-titanate system, which, due to perfect piezoelectric characteristics, is currently the main piezoelectric material.

Currently various fillers of raw stocks of piezoelectric ceramics are used to create pores in the specimens, mostly these are organic materials such as starch, corn flour, talc etc. [8–10], and inorganic fillers are, for example, aluminum oxide [10]. Such fillers are burnt at temperatures of around 500 °C. We suggested using [11,12] fine-disperse polystyrene, having pellet size of $\sim 2\,\mu$m, which assumes obtaining small-size pores evenly distributed in the specimen volume. Polystyrene has quite low decomposition temperature ($\sim$ 300−350 °C). Therefore, you can suggest that in process of piezoelectric ceramic specimens sintering the products of polystyrene decomposition are fully removed — styrene with boiling temperature of 145 °C. At the same time the studies of the porous ceramic potassium-sodium niobate (KNN) specimen structure demonstrated [12] that at percentage content of pores below 30 %, the pores have a closed volume inside rather dense granular structure of ceramics. It allows assuming that in process of sintering inside pores the residual vapors of styrene may be preserved, which, when cooled down to room temperature „is condensed“ on the inner surface of pores. Therefore, it is interesting to conduct benchmarking studies of disperse dependences of dielectric permittivity of porous KNN ceramic specimens and non-porous specimens.

In this paper solid-phase synthesis of materials $KNbO_3$ and $NaNbO_3$ to produce ceramics $(K_{0.5}Na_{0.5})NbO_3$ (KNN) was conducted in two stages to ensure maximum homogeneity of the composition. The first ones at temperature of 650 °C, the second one at temperature of 700 °C. At the stage of producing the stocks to achieve a volume share of pores in ceramic specimens, the correspondence of the mass and volume shares of the ceramic mixture and polystyrene was estimated. The stocks were produced from the estimate 0 (KNN), 10 (KNN10), 25 (KNN25) and 40 (KNN40) of pore volume percentages. The specimens were pressed in the form of tablets with a diameter of 10.4 mm and a thickness of 1−2 mm under 500 at. The sintering process was carried out in two stages. At the first one, at temperature of 350 °C, polystyrene was removed. Then the

stocks were sintered in a muffle furnace at temperature of 1100 °C for 4 h.

Samples of sodium niobate ceramics were synthesized and studied using the equipment of the Shared Research Facility at the Tver State University.

2. Dielectric permittivity dispersion

2.1. Experimental results

The studies of complex dielectric permittivity were carried out in a wide temperature range, from room temperature (~ 25 °C) to 450 °C.

Dielectric spectra were measured with a phase-sensitive Vector-175 LCR meter under continuous heating of the sample at a rate no greater than 1 degree per minute. This rate made it possible to record spectra in the range of 1 Hz−30 MHz within a time interval that did not exceed the duration of sample heating by one degree. Since measurements were carried out at temperatures up to 450 °C, the accuracy of 1 degree is quite high.

Text files of frequency dependences recorded by Vector-175 contain complete data on complex resistance, conductance, and capacitance that makes it possible to analyze temperature and dispersion dependences of complex dielectric characteristics.

For detailed analysis of relaxation processes in potassium-sodium niobate ceramics, we built complex dielectric permittivity diagrams $\varepsilon''(\varepsilon')$ using frequency dependences of complex dielectric permittivity measured using Vector-175. Several various relaxation processes may be identified in the diagrams (Figure 1).

In the area of low frequencies all specimens at all investigated temperatures have linear dispersion. To analyze linear dispersion (low frequency range) it is common to use empirical estimated reception [13], when the linear sections of diagrams $\varepsilon''(\varepsilon')$ are rebuilt into diagrams of dispersion of complex electric modulus $\beta''(\beta')$, which is estimated using the following formulas:

$$\beta' = \frac{\varepsilon'}{(\varepsilon')^2 + (\varepsilon'')^2} \tag{1}$$

$$\beta'' = \frac{\varepsilon''}{(\varepsilon')^2 + (\varepsilon'')^2}. \tag{2}$$

The corresponding diagrams for every studied specimen are also given in Figure 1.

In the comparatively high-frequency range (above 100 kHz) the circumference arcs or circumferences are observed. Such type of dielectric dispersion diagrams means, according to [14,15], the presence of both relaxation process and dispersion of resonance type. The first process, in case of a symmetrical semi-circumference arc is described by Cole-Cole theory, or, when the arc is asymmetrical, by Gavriljak-Negami theory.

At the same time, not all dielectric spectra of porous specimens allow to clearly define the diagram shape. For example, the circumference smoothly changes into the arc of another radius, there is no sharp transition between the straight line, which characterizes the section of linear dispersion, and the circumference arc corresponding to the relaxation process. Such behavior probably means the contribution of not one, but many processes in the dielectric response.

2.2. Mathematic simulation

To analyze dispersion dependences of complex dielectric permittivity, the mathematic simulation method was used, which we studied in detail previously [16,17].

In paper [17], we used Cole-Cole equation to model the relaxation processes. As it was shown above, the diagrams of porous ceramic KNN specimens dielectric permittivity dispersion, built using the experimental data, have asymmetrical arcs. Therefore, in this paper it was decided to use empirical equation of Gavriljak-Negami theory, where the equation denominator is additionally raised to power (γ). In case $\gamma = 1$ we have the equation of Cole-Cole theory. If in [17] we considered only the contribution to dielectric response of high frequency processes, in this paper we are interested in the entire studied frequency range. Therefore a term was added to the equation produced in paper [17], which characterizes the contribution of low-frequency conductivity considered in detail in [16].

As a result, in the general case the equation for dielectric response with account of existence of N relaxation processes (the first term), decay effects (the second term) and contribution of complex conductivity (the third and fourth terms) is as follows:

$$\varepsilon^*(\omega) = \varepsilon(\infty) + \sum_{n=1}^{N} \frac{\varepsilon_n(0) - \varepsilon(\infty)}{\left(1 + (i\omega\tau_n)^{1-\lambda_n}\right)^{\gamma}} + \frac{\varepsilon(0) - \varepsilon(\infty)}{1 - \left(\frac{\omega}{\omega_0}\right)^2 + i\Gamma\frac{\omega}{\omega_0}} - \frac{1}{\varepsilon_0}\tau_\sigma\sigma_\infty \frac{1 - i\omega\tau_\sigma}{1 + (\omega\tau_\sigma)^2} + \frac{1}{\varepsilon_0} iB\omega^{s-1}. \tag{3}$$

Here $\varepsilon(\infty)$ dielectric permittivity corresponding to infinite frequency, $\varepsilon_0 = 8.85 \cdot 10^{-12}$ F/m — dielectric constant, Γ — decay parameter, σ_∞ — conductivity at infinite frequency, $\tau_\sigma = 1/\omega_0$ — relaxation time of conductivity current, ω_0 — frequency of resonance polarization (determined by the maximum at frequency dependence of the real part of complex conductivity). This frequency corresponds to the maximum of the frequency dependence of the real part of complex conductivity. τ_n, where $n = 1, 2, \ldots, N$ — relaxation times of various relaxation processes. Accordingly, $\lambda_n = 2\psi/\pi$ is the width of the relaxation time spectrum of each process, ψ is the opening angle of the diagram arc $\varepsilon''(\varepsilon')$, $\varepsilon_n(0)$ and $\varepsilon_n(\infty)$ — specify the maximum and minimum dielectric permittivity for each process with $\varepsilon_{n+1}(0) = \varepsilon_n(\infty)$, and $\varepsilon_n(\infty) = \varepsilon_N(\infty)$ (see [17] for detail). When the dielectric response follows the empirical Debye law characterizing the contribution of

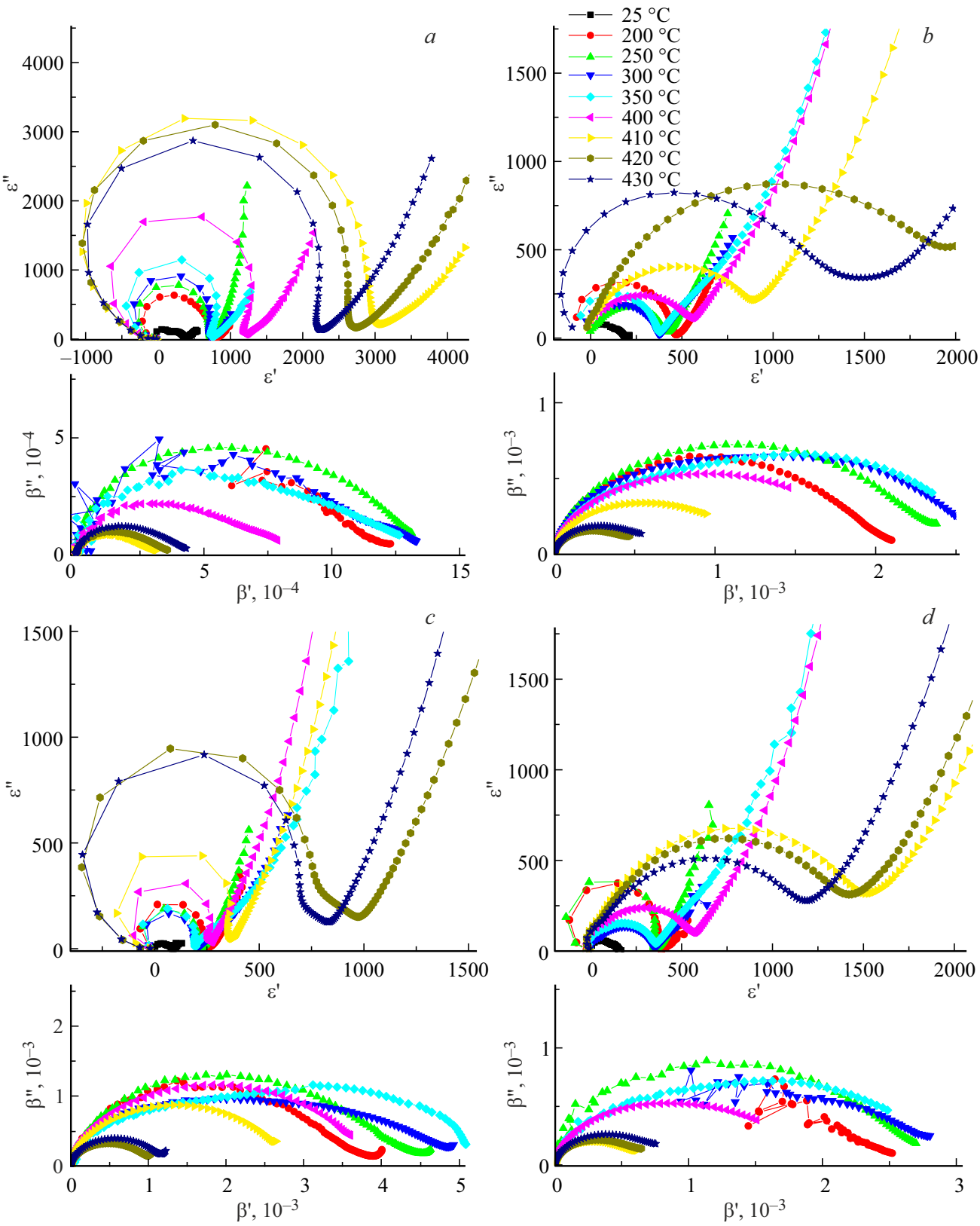

Figure 1. Diagrams of dielectric permittivity dispersion (top) and electric modulus (borrom) of KNN specimens(*a*), KNN10 (*b*), KNN25 (*c*) and KNN40 (*d*).

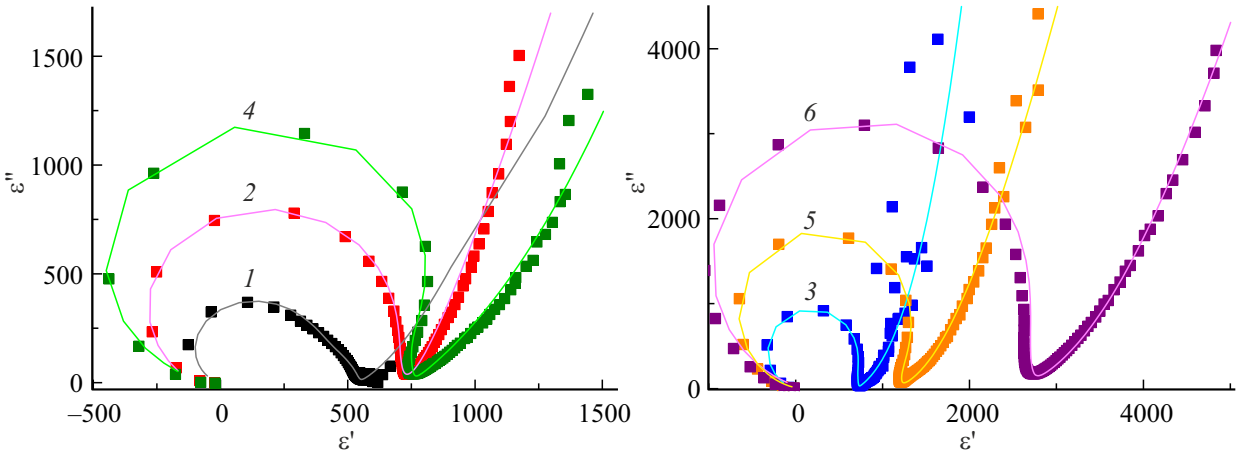

Figure 2. Dielectric permittivity dispersion diagrams for KNN ceramic specimen without pores. Symbols — experiment, solid lines — simulation result. Temperatures: *1* — 150 °C, *2* — 250 °C, *3* — 300 °C, *4* — 350 °C, *5* — 400 °C, *6* — 420 °C.

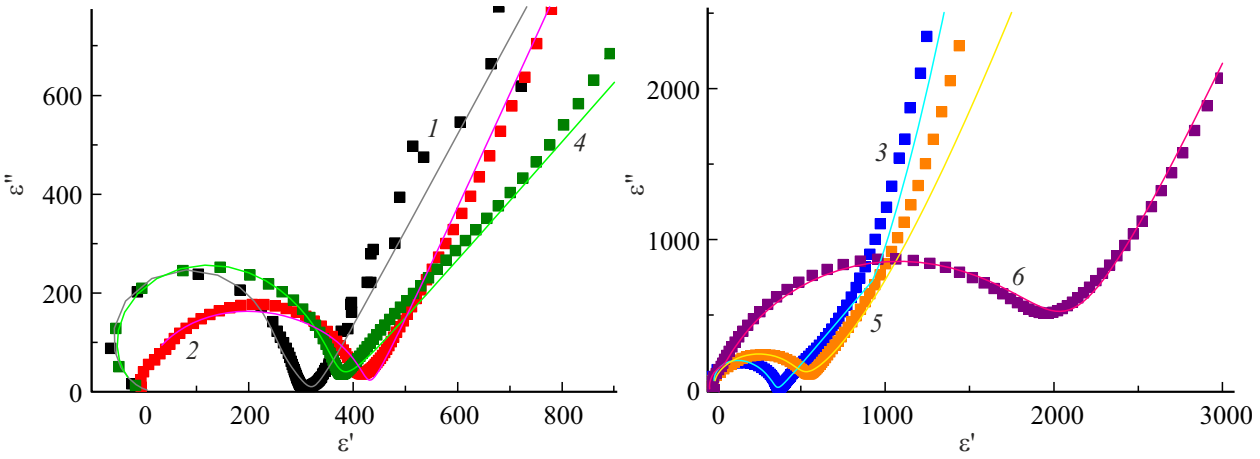

Figure 3. Dielectric permittivity dispersion diagrams of KNN10 ceramic specimen. Symbols — experiment, solid lines — simulation result. Temperatures: *1* — 150 °C, *2* — 250 °C, *3* — 300 °C, *4* — 350 °C, *5* — 400 °C, *6* — 420 °C.

an ordered subsystem to the dielectric response, $\lambda = 0$. When the dielectric response is governed by a disordered subsystem (which corresponds to the empirical Cole-Cole or Gavriljak-Negami law), then $\lambda \neq 0$. In the last term B — constant determining the frequency independent component of conductivity, s — parameter characterizing the angle of inclination of rectilinear sections at frequency dependence of the real part of complex conductivity in logarithmic scale [14].

If the fourth term characterizes contribution to the dielectric response of the low frequency conductivity processes, the third term characterizes the relaxation conductivity that occurs at higher frequencies.

To build dispersion diagrams using mathematic simulation, formula (3) was used to calculate the real and imaginary parts of the complex dielectric permittivity. When one determines the imaginary part of complex permittivity, it should be taken into account that negative dielectric losses contradict the fundamental laws of physics; therefore, $\varepsilon''(\omega) = |\mathrm{Im}(\varepsilon^*(\omega))|$. The modulus sign is applied separately to each contribution (term of Eq. (3)) to complex dielectric permittivity.

Using formula (3), we calculated the dielectric response of KNN ceramic specimens with and without pores (Figures 2–5) for various temperatures. The parameters required for the calculation were found from the experimental data using the method we considered in detail in papers [16] and [17]. As you can see, at relatively higher frequencies, in the area of relaxation and resonance dispersions a very good match is observed between the results of mathematic simulation and experimental data. At the same time in the area of linear dispersion, at the frequencies below 100 Hz, the angle of inclination of the estimated curve and the curve observed in the experiment may differ.

This deviation is especially significant for porous specimens. Most likely, the specimens with pores in the low-frequency area include additional relaxation processes, which we did not take into account in the equation (3).

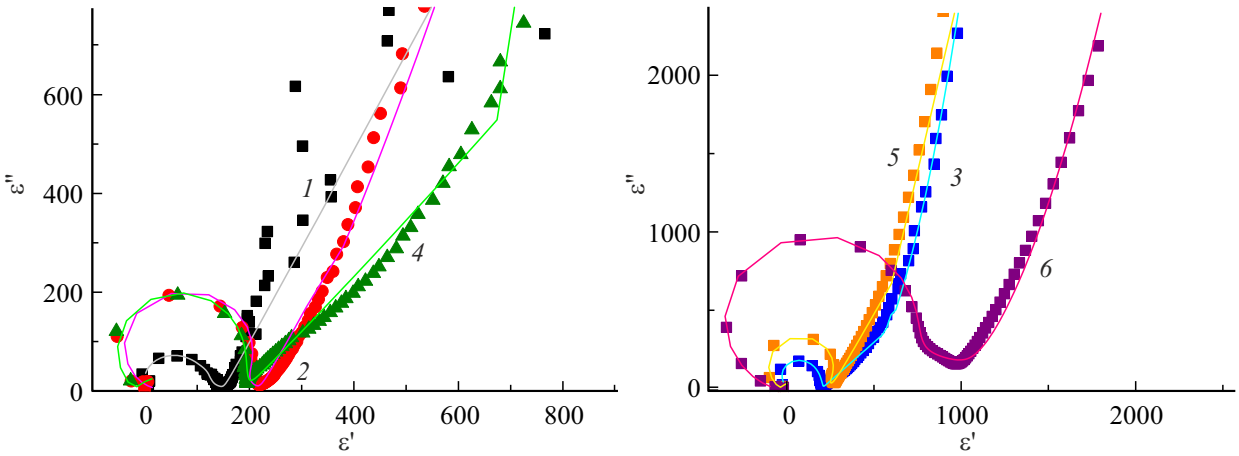

Figure 4. Dielectric permittivity dispersion diagrams for KNN25 ceramic specimen. Symbols — experiment, solid lines — simulation result. Temperatures: *1* — 150 °C, *2* — 250 °C, *3* — 300 °C, *4* — 350 °C, *5* — 400 °C, *6* — 420 °C.

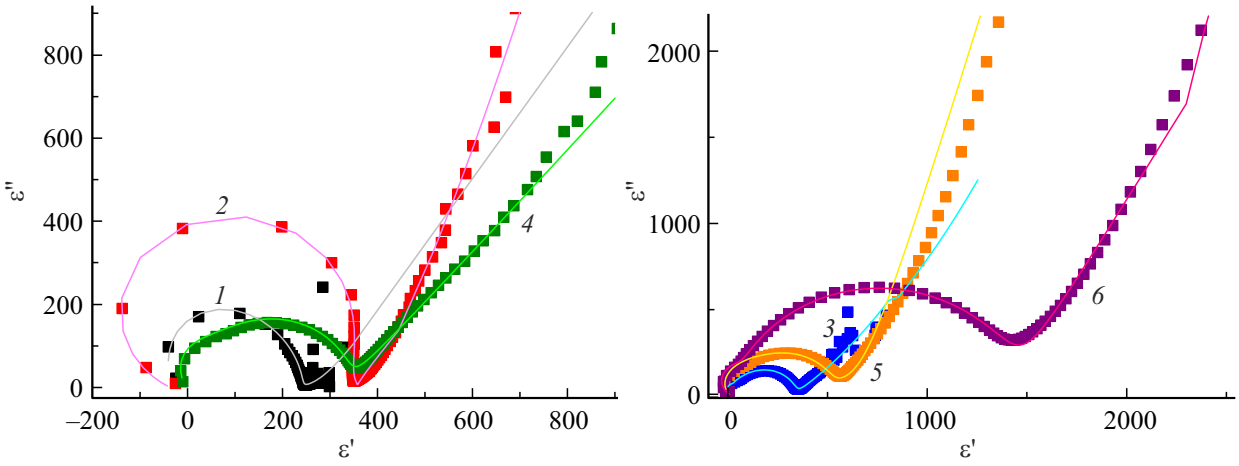

Figure 5. Dielectric permittivity dispersion diagrams of KNN40 ceramic specimen. Symbols — experiment, solid lines — simulation result. Temperatures: *1* — 150 °C, *2* — 250 °C, *3* — 300 °C, *4* — 350 °C, *5* — 400 °C, *6* — 420 °C.

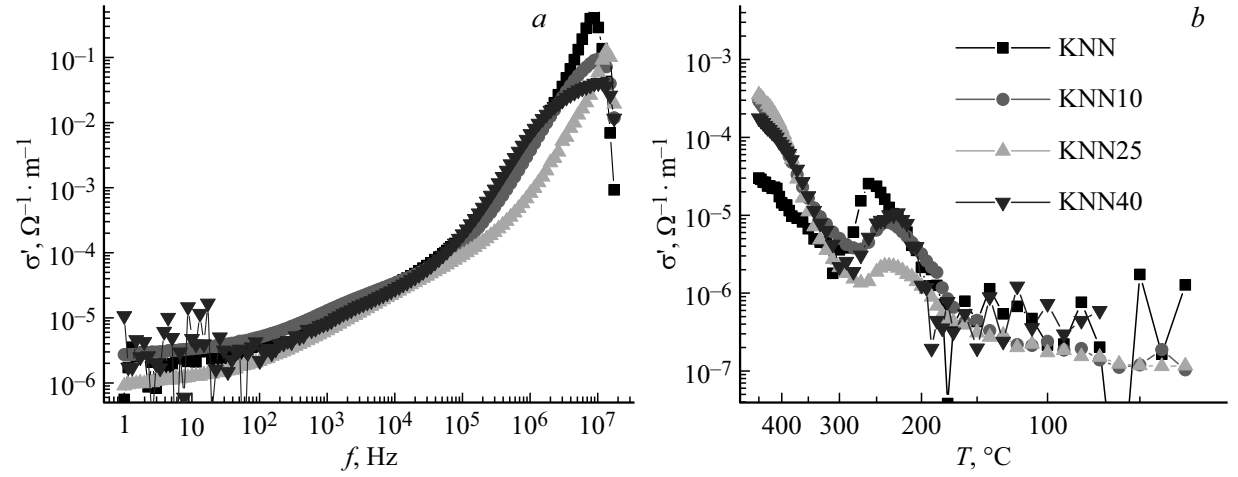

Figure 6. Frequency (*a*) and temperature (*b*) dependences of the real part of complex conductivity of KNN, KNN10, KNN25 and KNN40 specimens. *a* — measurement temperature 300 °C, *b* — measurement frequency 100 Hz.

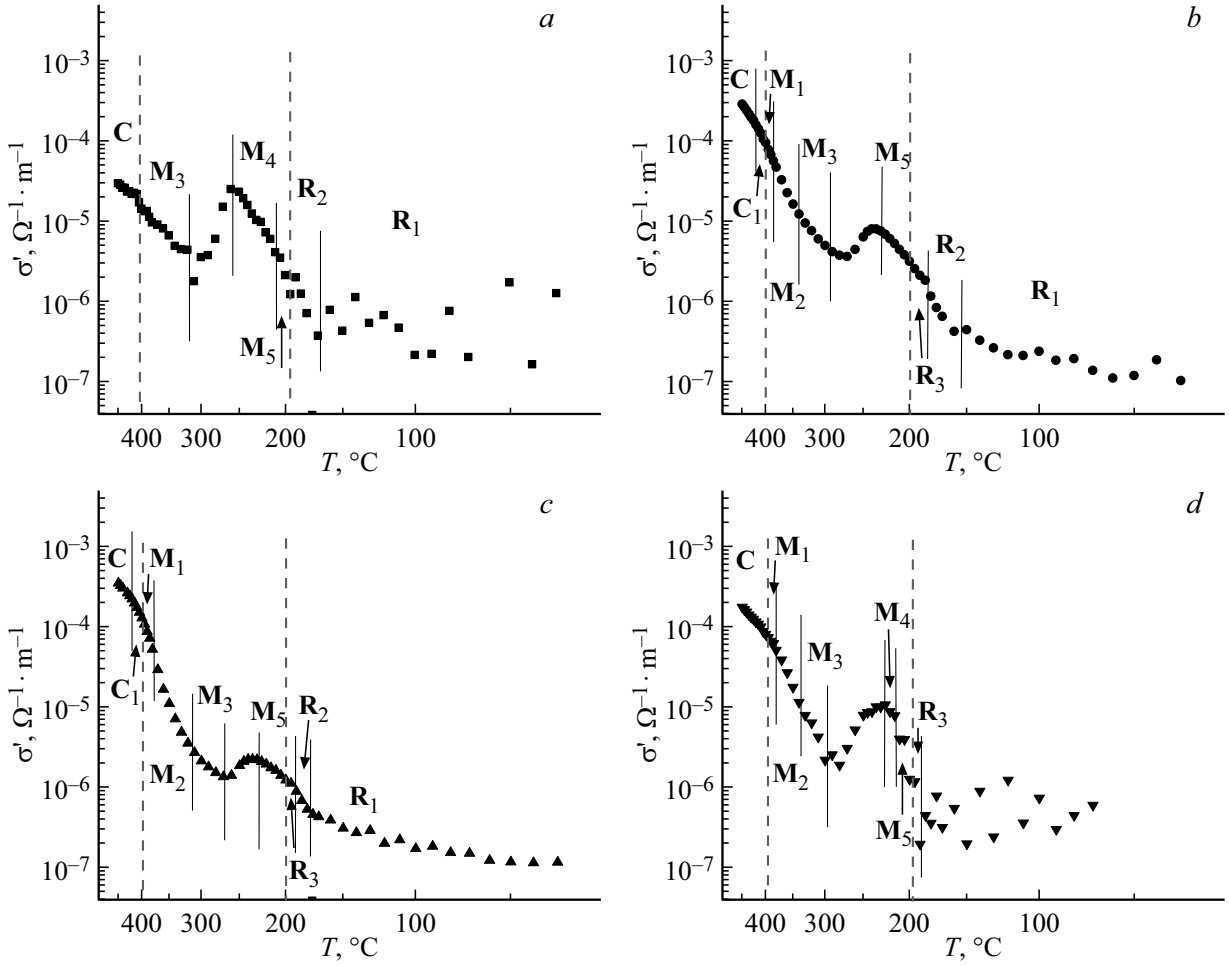

Figure 7. Temperature dependences of real part of complex conductivity of ceramics KNN (*a*) KNN10 (*b*), KNN25 (*c*), KNN40 (*d*). Measurement frequency is 100 Hz. Dotted lines show SPT temperatures: rhombic (**R**) ferroelectric phase — monoclinic (**M**) ferroelectric phase ($T_t = 200\,^\circ$C); monoclinic (**M**) ferroelectric phase — cubic (**C**) paraelectric phase ($T_c = 400\,^\circ$C) (data on SPT is given according to [18]).

Comparative analysis of the relaxation times calculated both for high-frequency (relaxation polarization and relaxation conductivity) and for low-frequency (migration polarization) processes found no significant differences for the specimens with and without pores. At the same time, mathematic simulation demonstrated that the contribution of relaxation conductivity to the dielectric response present in all porous KNN specimens, in a specimen without pores only occurred in the temperature interval: $200\,^\circ\text{C} < \text{T} < 400\,^\circ$C, which, according to [18], corresponds to the monoclinic crystalline structure of ceramics $(K_{0.5}Na_{0.5})NbO_3$. Most likely, structure rebuild from the rhombic phase to the monoclinic one, happening at temperature $\sim 200\,^\circ$C, causes formation of additional charge states, which may contribute to the conductivity.

It should be noted that in the experiment, at low frequencies (up to 100–300 Hz) and temperatures of up to $350\,^\circ$C for the specimen without pores, and up to $\sim 250\,^\circ$C for the porous specimens, a significant spread was observed in the values of dielectric permittivity supported by the contribution to the dielectric response of migration polarization. These points were removed from the graphic representation (Figures 2–5). The fact that oscillations of charges being the cause for migration polarization become less in the porous specimens may indicate the stabilizing role of charge states on the inner surface of the pores. Thus, it is entirely possible that the charges are „fixed“ on the traps of surface levels. Existence of such additional energy levels must also contribute to the conductivity processes.

Therefore, it became interesting to do additional analysis of frequency and temperature dependences of the complex conductivity.

3. Conductivity

To check the issue of conductivity contribution to dispersion dependences of dielectric permittivity and its potential impact at relaxation dielectric processes, according to the data received using a phase sensitive LCR meter

Energy of KNN image activation estimated for different tempersture intervals according to Figure 7

Sample	Energy of activation, eV									
	C	C_1	M_1	M_2	M_3	M_4	M_5	R_3	R_2	R_1
KNN	0.68	–	1.38			1.87	4.05	4.82		0.22
KNN10	1.68	2.04		2.55	1.29	1.37			1.67	0.21
KNN25	1.29	1.95	2.9	2.76	1.05	0.82			1.84	0.23
KNN40	1.30			2.38	2.41	1.32	3.9		–	–

VECTOR-175, the frequency and temperature (Figure 6) dependences were built for the real part of complex conductivity $\sigma'(f)$. Frequency dependences for all temperatures are practically similar (curves (Figure 6,*a*) show dependences for temperature 300 °C). In all compositions the dependence includes nonlinear and linear sections, one of which is practically parallel to the horizontal axis and is incident upon the area of low frequencies up to ~ 200 Hz. This means that all specimens have conductivity similar to DC conductivity, i. e. frequency independent one. Using temperature dependences, built for this frequency range, it is possible to calculate the activation energy of charge carriers localized on the surface level traps.

Since the activation energy of conductivity processes related to additional energy levels is taken into account only for DC conductivity, frequency 100 Hz was chosen for the calculation (Figure 6, *b*).

You can see well the difference in the progress of conductivity for the specimen without and with pores in the temperature dependence of conductivity (Figure 6, *b*). At temperatures below 200 °C in the specimen without pores and KNN40 there is a spread of conductivity values similar to the spread observed in the dependences of dielectric permittivity. Much lower conductivity value at high temperatures (above 350 °C) in the specimen without pores, according to the porous specimens, attracts attention. The possible explanation of this experimental fact is the following: as noted in the introduction, the dense granular structure of KNN ceramic may hold styrene vapors inside the pores in process of sintering, which then, in process of cooling, are condensed in the inner surface of the pores, and when the specimens are heated, polystyrene remains are again decomposed, and above temperature 350 °C the vapors of styrene containing OH^- group may additionally contribute to the conductivity processes. This assumption agrees well with the recorded fact of partial deviation of the modeling results for the dielectric response of porous specimens with the experimental data, which was mentioned above.

In the temperature interval 250–300 °C all specimens show a conductivity surge, which in the semiconductor physics is related to depletion of admixture levels. Since KNN ceramic is not a semiconductor, such behavior may be related to depletion of surface energy levels. Such levels in the ceramics most likely occur in the grain boundaries, and in porous specimens also on the inner surface of pores.

Temperature dependences of the real part of conductivity $\sigma'(1/T)$ were built from reverse temperature on a logarithmic scale (Figures 6, *b*, 7). The curve, for convenience of analysis, shows temperature (in °C), corresponding to values $1/T$ (in 1/K). Such building makes it possible to calculate the conductivity process activation energy in inclined rectilinear sections of temperature dependences of the real part of complex conductivity described by Arrhenius law:

$$\sigma = \sigma_0 \exp\left(-\frac{E_a}{2kT}\right), \tag{4}$$

where E_a — activation energy, σ_0 — pre-exponential factor, k — Boltzmann constant.

Values E_a were calculated for each temperature interval noted by vertical lines in Figure 7 (vertical dotted lines show temperatures of structural phase transitions (SPT)), letters correspond to the crystallographic structure of temperature phase. These results are given in Table.

As expected [15], the specimen without pores in case of SPT of rhombic — monoclinic phase experiences electric conductivity surge, and in case of SPT of cubic — rhombic phase the linear section inclination varies. At the same time in porous specimens the changes in the inclinations of linear sections of the temperature dependence of electric conductivity in Arrhenius coordinates do not match SPT temperatures, and the number of linear sections increases, compared to the specimen without pores. As a result, the porous specimens have more diverse activation energies (Table).

Since the change of the activation energy means the change of the electric conductivity mechanism, then, according to the data in the table, the porous specimens have additional mechanisms of electric conductivity, which are unavailable in the specimen without pores.

4. Conclusion

A comparative analysis of the dispersion diagrams of complex permittivity within the 10 Hz–20 MHz frequency range revealed an almost complete correspondence between

the proposed mathematical model and experimental data. Partial deviations of the simulation results from the experiment for the porous specimens are explained by the fact that the equation used to simulate dielectric response did not take into account the contribution to the conductivity of charges localized on the surface levels of the internal surface of pores.

It was found that introduction of KNN pores into the ceramics, despite the minor change of the dielectric permittivity dispersion mechanisms, causes appearance of additional mechanisms of complex conductivity, which is indicated by the increase in various activation energies in porous specimens. Since, as author of [19] has shown, the spread of activation energy values may be due to the chaos of the admixture (structure defect) distribution chaos, and pores may be deemed defects to a certain degree, their presence will result in a higher number of different activation energies in the porous specimens compared to a specimen without pores.

Conflict of interest

The authors declare no conflict of interest.

References

[1] W. Wersing, K. Lubitz, J. Mohaupt. Ferroelectrics **68**, *1*, 77 (1986).
[2] A.N. Rybyanets, D.I. Makarev, N.A. Shvetsova. Ferroelectrics **539**, *1*, 101 (2019).
[3] J. Rödel, K.G. Webber, R. Dittmer, W. Jo, M. Kimura, D. Damjanovic. J. of the European Ceramic Society **35**, *6*, 1659 (2015).
[4] B. Malič, A. Benčan, T. Rojac, M. Kosec. Acta Chimica Slovenica. **55**, *4*, 719 (2008).
[5] J. Wu, D. Xiao, J. Zhu. Chemical Reviews **115**, *7*, 2559 (2015).
[6] O.V. Malyshkina, E.S. Tesnikova, N.E. Malysheva, A.I. Ivanova. Fiziko-khimicheskiye aspekty izucheniya klasterov, nanostruktur i nanomaterialov. **11**, 198 (2019). (in Russian).
[7] A.N.Reznichenko, M.A. Lugovaya, E.I. Petrova, N.A. Shvetsova A.N. Rybyanets. Ferroelectrics **539**, *1*, 93 (2019).
[8] Y. Li, C. Wei, G. Lunlun, Ruifang Zhang, Xudong Cheng. High Temp. Mater. Processes. **35**, *9*, 955 (2016).
[9] J.G. Ayala-Landeros, V. Saucedo-Rivalcoba, S. Bribiesca-Vasquez, V.M. Castaño, A.L. Martínez-Hernández, C. Velasco-Santos. Science of Sintering **48**, *1*, 29 (2016).
[10] S.E. Gass, M.L. Sandoval, M.H. Talou, A.G.T. Martinez, M.A. Camerucci, E. Gregorová, W. Pabst. Procedia Materials Science **9**, 254. (2015).
[11] O.V. Malyshkina, E.V. Barabanova, N.E. Malysheva, A. Kapustkin, A.I. Ivanova. Ferroelectrics **561**, *1*, 114 (2020).
[12] D.V. Mamaev, O.V. Malyshkina, A.I. Ivanova. Fiziko-khimicheskiye aspekty izucheniya klasterov, nanostruktur i nanomaterialov. **16**, 219 (2024). (in Russian).
[13] N.M. Galiyarova. V sb. Segnetoelektriki i piezoelektriki. Tver: Izd-vo TGU. 98 (1991). (in Russian).
[14] A.K. Jonscher. Universal relaxation law: a sequel to Dielectric relaxation in solids. Chelsea Dielectrics Press Limited, London. (1996). 415 p.
[15] Yu.M. Poplavko. Fizika dielektrikov. Vishcha shkola. Golovnoe izd-vo, Kiev. (1980). 400 s. (in Russian).
[16] N.E. Malysheva, E.V. D'yakova, O.V. Malyshkina. Fiziko-khimicheskiye aspekty izucheniya klasterov, nanostruktur i nanomaterialov. **15**, 481 (2023). (in Russian).
[17] O.V. Malyshkina, N.E. Malysheva, E.V. Dyakova, M. Ali. FTT **66**, *8*, 1384 (2024). (in Russian).
[18] B. Yaffe, W. Cook, G. Yaffe. Piezoelektricheskaya keramika. Mir, Moskva. (1974). 288 s. (in Russian)
[19] Galiyarova, N.M. Dielektricheskaya spektroskopiya segnetoelektrikov, fraktalnost i mekhanizmy dvizheniya domennykh i mezhfaznykh granits: Diss. dok. fiz. mat. nauk. Voronezh State University, 2006.

Translated by M.Verenikina

i